

# IMPACT OF SYSTEMATICS ON SZ-OPTICAL SCALING RELATIONS

T. BIESIADZINSKI<sup>1</sup>, J. MCMAHON<sup>1</sup>, C. MILLER<sup>2</sup>, B. NORD<sup>1</sup> AND L. SHAW<sup>3</sup>

<sup>1</sup>Physics Department, University of Michigan, Ann Arbor, MI 48109

<sup>2</sup>Astronomy Department, University of Michigan, Ann Arbor, MI 48109

<sup>3</sup>Physics Department, Yale, New Haven, CT 06511

*Submitted to ApJ letters*

## ABSTRACT

One of the central goals of multi-wavelength galaxy cluster cosmology is to unite all cluster observables to form a consistent understanding of cluster mass. Here, we study the impact of systematic effects from optical cluster catalogs on stacked SZ signals. We show that the optically predicted  $Y$ -decrement can vary by as much as 50% based on the current  $2\sigma$  systematic uncertainties in the observed mass-richness relationship. Mis-centering and impurities will suppress the SZ signal compared to expectations for a clean and perfectly centered optical sample, but to a lesser degree. We show that the level of these variations and suppression is dependent on the amount of systematics in the optical cluster catalogs. We also study luminosity-dependent sub-sampling of the optical catalog, which creates Malmquist-like effects that biases upwards the observed  $Y$ -decrement of the stacked signal. We show that the current Planck measurements of the  $Y$ -decrement around SDSS optical clusters and their X-ray counterparts are consistent with expectations after accounting for the  $1\sigma$  ( $2\sigma$ ) optical systematic uncertainties using the Johnston (Rozo) mass richness relation.

*Subject headings:* clusters: general — clusters: cosmology — clusters: SZ, Optical, X-ray — clusters: scaling relations — stacking

## 1. INTRODUCTION

Measurements of the abundance of galaxy clusters as a function of their masses and redshift provides an important constraint on the nature of dark matter and dark energy (e.g., Vikhlinin et al. 2009; Vanderlinde et al. 2010; Sehgal et al. 2011). Joint analysis of multi-wavelength observations, including optical cluster catalogs and their Sunyaev-Zel'dovich (SZ– Sunyaev & Zeldovich 1972; Birkinshaw 1999; Carlstrom et al. 2002) counterparts, will help realize the full cosmological potential of galaxy clusters (Cunha et al. 2009; Rozo et al. 2009; Wu et al. 2010).

Optical galaxy cluster surveys have identified thousands of clusters down to a mass limit of  $\sim 10^{14} M_{\odot}$  (e.g., the maxBCG catalog of SDSS clusters, Koester et al. 2007a), and millimeter wave surveys have discovered hundreds of clusters using the SZ effect (e.g., Vanderlinde et al. 2010; Williamson et al. 2011; Marriage et al. 2011; Ade et al. 2011a), albeit to a higher mass limit due to instrumental noise. Using these catalogs, researchers apply *mass-observable relations* to relate the true underlying halo mass to observed properties, like the galaxy member count in the optical (richness,  $N_{gal}$  or  $N_{200}$ ) or the SZ decrement ( $y$  or  $Y_{500}$ ).

One can probe scaling relations down to masses below the detection limit by stacking the signal around known clusters. For instance, stacking has been used to the great benefit of mass calibration in weak lensing and X-ray studies (Sheldon et al. 2007; Rykoff et al. 2008). Similarly, the SZ/X-ray cluster scaling-laws and pressure-profiles were evaluated by Komatsu et al. (2011) and Melin et al. (2011), who stacked the SZ signal from WMAP data around known optical/X-ray clusters. These joint optical/X-ray/SZ analyses allow researchers to take advantage of the large volumes and mass ranges

from optical cluster catalogs in combination with the lower scatter in the mass observable relation in X-ray/SZ catalogs (Shaw et al. 2008; Nagai et al. 2006; Rasia et al. 2011; Motl et al. 2005).

The SZ signal recovered from stacking Planck data at positions of the maxBCG (Koester et al. 2007a) clusters shows a deficit of SZ signal compared to what is expected from current mass-richness scaling relationships (Aghanim et al. 2011a); this discrepancy has been confirmed using WMAP data (Draper et al. 2011). This discrepancy manifests itself differently for two mass-richness calibrations (Johnston et al. 2007; Rozo et al. 2009) both of which are based on the Sheldon et al. (2007) stacked weak-lensing stacked mass measurements of the maxBCG clusters. For the Johnston et al. (2007) calibration, a simple reduction in the global weak-lensing mass calibration by 25% would eliminate the discrepancy. The Rozo et al. (2009) mass calibration requires a larger correction and a scaling law that is not self-similar. Aghanim et al. (2011a) also show that a subset of the maxBCG clusters with measured X-ray luminosities from the MCXC catalog (Piffaretti et al. 2011) can match the predicted  $Y_{500}$  vs. richness scaling relationship, although they did not consider selection effects inherent in such a hybrid catalog. Aghanim et al. (2011a) argue that the X-ray and SZ properties of cluster gas halos are more stably related to each other than either are to the optical richness.

The Aghanim et al. (2011a) analysis was based on a comparison of the observed  $Y_{500}$  around maxBCG clusters to two models with different mass-richness calibrations and without including optical systematics. They evaluated the impact of impurities in the optical catalog as well as scatter in the mass-richness relations and concluded that neither could account for the observed discrepancy individually. Here, we broaden the

Aghanim et al. (2011a) analysis to include the *uncertainties in the mass calibrations* as well as the *combined systematic effects* in optical cluster catalogs. Instead of two model predictions to compare against the data, we look at the family of predictions which come from uncertainties in the calibrations and the ranges of systematics in optical cluster catalogs.

There are numerous systematic effects in optical galaxy cluster catalogs. These include the cluster selection (as a function of mass  $M$  and redshift  $z$ ) which encompasses: *completeness*—the probability that a true halo will be detected; and *purity*—the probability that a detection correctly identifies a halo rather than noise (e.g., Miller et al. 2005). Cluster *redshifts* estimated using photometric data are uncertain which introduces scatter in the observed redshift. There is uncertainty in the *mass-richness* calibration as well as *scatter*. Finally, misidentification of BCGs in the maxBCG cluster-finder produces angular offsets between true and recovered *cluster centers* (Johnston et al. 2007) called *mis-centering*. Centering offsets driven by other mechanisms (e.g., astrophysical: Sanderson et al. 2009) are smaller than those caused by the BCG mis-identification, and so we do not consider them in this study.

Using mock clusters taken from N-body simulations, we directly manipulate the purity, mass-scatter, scaling calibrations and their uncertainties. We then re-create the Planck richness stacking technique on these mock catalogs to create model  $Y_{500}$ -richness relations and compare to the Planck observations. In §2, we describe the N-body simulations and the suite of simulated optical cluster catalogs with various systematics, the mock Planck SZ observations, the mock X-ray observations and the stacking procedure. We then show the results of stacking the SZ signal for each systematic to explore how each systematic can individually affect of the SZ signal (§3), and we compare to the Planck joint SZ-optical and X-ray analyses (§3.1). Throughout this paper, we assume a  $\Lambda$ CDM cosmology with a  $\Omega_\Lambda=0.7$  and  $H_0=0.71$  unless otherwise noted.

## 2. SIMULATIONS

We begin with the mass function and halo positions from an N-body simulation. We then impose observables and realistic systematic effects to produce mock optical catalogs and then dress the halos with gas and simulate Planck SZ observations.

### 2.1. N-body Lightcone

To generate the mock SZ maps and galaxy catalogs, we begin with the output of a large ( $N = 1260^3$  particles,  $1000 [\text{Mpc } h^{-1}]^3$ ) cosmological dark matter simulation. Cosmological parameters were chosen to be consistent with those measured from the five-year *WMAP* data (Dunkley et al. 2009) combined with large-scale structure observations, namely  $\sigma_8 = 0.8$ ,  $\Omega_M = 0.264$  and  $\Omega_b = 0.044$ . The simulation was carried out using the tree-particle-mesh code of Bode & Ostriker (2003). In total, the lightcone covers a single octant on the sky ( $\sim 5000 \text{ deg}^2$ ) to a redshift of 3, containing halos with masses  $M_{\text{FOF}} > 3 \times 10^{13} h^{-1} M_\odot$ . With the mass resolution available from this simulation we can reproduce the properties of the maxBCG catalog, including systematics, for clusters with  $M_{500} > 6 \times 10^{13} h^{-1} M_\odot$

or  $N_{200} > 20$ . The simulation does not provide any observables (e.g., richness or SZ/X-ray luminosity) and so in the next sub-sections we describe how the mock “observed” catalogs are created.

### 2.2. Optical Cluster Catalogs

In the Planck analysis (Aghanim et al. 2011a), the clusters are binned according to their optical richness ( $N_{200}$ ). Recall, that richness is an observed quantity and at any fixed value clusters can have a range of true masses (the *mass scatter*). Richness  $N_{200}$  (or  $N_{\text{gals}}$ ) is defined as the number of bright red galaxies (within the E/S0 ridgeline) inside  $R_{200}$  that are brighter than  $0.4 L^*$  (Koester et al. 2007a). Using our simulated halo catalog we apply an iterative technique that imprints the mass-richness relations and their scatter directly onto the halos. In this process, the original halo masses have to be slightly adjusted in order to match the published scatter in  $M_{\text{true}}$  at fixed richness such that the abundance goes from  $n(M_{\text{true}})$  to  $n(M_{N_{200}})$ . We then create mock cluster catalogs by adjusting the following systematic parameters:

**Mass-richness Calibration:** We define the richnesses of the halos according to equation 26 from Johnston et al. (2007) with  $(M_{200}|N_{200} = (8.8 \pm 0.4_{\text{stat}} \pm 1.1_{\text{sys}}) \times 10^{13} h^{-1} M_\odot$  and  $\alpha_N = 1.28 \pm 0.04$ ) and equation 4 from Rozo et al. (2009) (with  $\alpha_{M|N} = 1.06 \pm 0.08_{\text{stat}} \pm 0.08_{\text{sys}}$  and  $B_{M|N} = 0.95 \pm 0.07_{\text{stat}} \pm 0.10_{\text{sys}}$ ). We look at one and two  $\sigma$  deviations from these mass calibrations. Masses are converted from  $M_{200}$  to  $M_{500}$  assuming an NFW profile and mass concentrations from Duffy et al. (2008), and are relative to the critical density.

**Completeness:** We vary the fraction of halos in bins of redshift and mass.

**Purity:** We add into the halo catalogs an additional number of false halos in bins of mass and redshift to create samples with different purities. We either vary the purity as a constant with mass and redshift or match the published maxBCG purity Koester et al. (2007a).

**Redshifts:** We scatter the true halo redshifts by normal distributions with varying widths as large as  $\sigma_z = 0.02$ .

**Center Offsets:** We offset the center for a fraction of the clusters according to Eq. 10 in Johnston et al. (2007). For the offset clusters, the actual amount of the offset is described by Eq 8 in Johnston et al. (2007). See also Figures 4 and 5 in Johnston et al. (2007).

**Mass Scatter** We vary the width of the log-normal distribution of masses at fixed richness.

Realizations of mock optical cluster catalogs are created from the halo catalogs including the above systematics. We apply completenesses, purities, and mis-centering fractions that are constant with redshift and mass (or richness). We also create maxBCG-like mock catalogs where we ensure that the completeness, purity, mis-centering fractions, and mass scatter match the relationships shown in Koester et al. (2007a), Koester et al. (2007b), Johnston et al. (2007) and Rozo et al. (2009). For instance in our maxBCG-like mocks, the fraction of incorrectly centered clusters ranges from 12% in the highest richness bins to 39% in the lowest richness bins with a mean offset of  $0.6 \text{ Mpc}$  corresponding to  $3'$  for a cluster at the mean redshift of

$z = 0.2$ ; the completeness and purity are  $>90\%$  above  $M_{500} > 1 \times 10^{14} h^{-1} M_{\odot}$  and have an estimated uncertainty of 2.5%; the mass scatter varies by 0.45 by  $\pm 0.10$ , similar to Rozo ( $\sigma_{\ln(M)|N_{200}} = 0.45^{+0.20}_{-0.18}$  (95% CL) at  $N_{200} \approx 40$ ).

### 2.3. Mock SZ Sky Maps and the Stacked Signal

The halo SZ signals are generated using a thermal pressure profile suggested by (Arnaud et al. 2010) and used in the Planck maxBCG stacking analysis (Aghanim et al. 2011a). Bonamente et al. (2011) compares the pressure profiles of 25 massive relaxed clusters observed in X-ray and with the Sunyaev-Zel’dovich Array (SZA) and find that they agree well with the Arnaud et al. (2010) profile up to  $R_{500}$ . We project the profile along the line-of-sight to produce a Compton-Y profile, scaled to the appropriate size for each halo redshift, the same process used in (Aghanim et al. 2011a). Mock *Planck* observations were created in each frequency band using the appropriate beam sizes, instrument noise and primary CMB (Ade et al. 2011a) temperature anisotropy. We concluded that the 143 GHz channel reproduced the dominant features of the multi-frequency analysis, and so we restricted our analysis solely to this channel, which has a beam size of 7.18 arcminute FWHM and a noise of  $0.9 \mu K$ -degree.

At the position of each optical cluster, we extracted the integrated thermal SZ signal  $Y_{500}$  from each SZ sky map using a matched filter (e.g., Herranz et al. 2002; Melin et al. 2006) with an Arnaud profile (Arnaud et al. 2010), the size of which is inferred from either the *Johnston* or *Rozo* richness-mass scaling relations (same as used in Aghanim et al. 2011a). We stacked these matched filtered signals in richness bins; then the amplitude is calibrated by comparing the spherical  $Y_{500}$  of the halos with the amplitude in the stacked SZ signal in the absence of systematics. We found that including an intrinsic scatter of 25% in  $Y_{500} - M_{500}$  (Shaw et al. 2008) did not affect our results beyond increasing statistical uncertainties in individual catalog realizations and so we did not include this additional scatter in the following analysis.

### 2.4. maxBCG-MCXC Subsample

The Planck team studied a subset of the maxBCG catalog whose positions were matched to within  $\sim 3$  arcminutes of X-ray clusters from the MCXC catalog (Piffaretti et al. 2011). Starting with the masses of our simulated haloes we assign X-ray luminosities ( $L_X$ ) and scatter according to Table 1 in Arnaud et al. (2010). We confirm that the scatter in the  $L_X$  scaling relations (at fixed mass and richness) are what is observed in Rozo et al. (2009), where  $\sigma_{\ln(L)|M}$  ranges from 0.5 at low mass to 0.45 at high mass and  $\sigma_{\ln(L)|N}$  is a constant 0.85 at all richnesses. We then select subsets of the simulated halos which have the same redshift and  $L_X$  distribution as the MCXC subsample. This allows us to reproduce the MCXC subsample without needing to know the exact selection function which is undoubtedly complex as this catalog is drawn from heterogeneous X-ray data. We also ensure that the mis-centering for this mock MCXC-maxBCG catalog is truncated at  $3'$ . It is important to note that the maxBCG-MCXC mock catalogs need not have the same scatter in the mass-richness relation as we

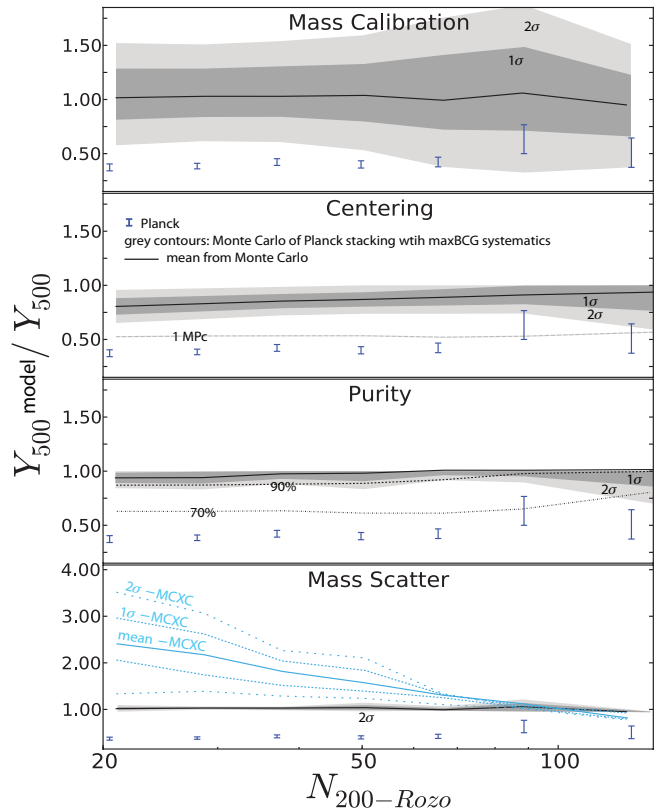


FIG. 1.— A comparison of the stacked  $Y_{500}$  in our family of mock cluster catalogs to a single “perfect” cluster catalog that has been calibrated according to Rozo et al. (2009). The solid black lines show the model with maxBCG-like systematics included (individually). The grey bands show the range of models after we include the 1 and 2  $\sigma$  uncertainties on the individual optical systematics. Grey dotted lines show more general models, while the blue lines in the bottom panel are specific to the maxBCG/MCXC sub-sample. The error bars are the Planck data. Uncertainty in the mass calibration is the dominant effect on the model predictions, however impurity and mis-centering both bias the model predictions towards lower values of  $Y_{500}$ . On the other hand, X-ray luminosity selected sub-samples (e.g., the MCXC) show highly biased  $Y_{500}$  predicted values (compared to a perfect optical catalog). See Figures 2 and 3 for the combined effects of these systematics.

imprinted into the full maxBCG mock samples. This is because we imprint the observed scatter from Arnaud et al. (2010) directly onto the full catalog and then draw a sub-sample. For the MCXC/maxBCG mock subsamples,  $\sigma_{\ln(L)|N}$  drops to 0.70 and  $\sigma_{\ln(M)|N_{200}}$  drops to 0.40.

## 3. RESULTS

In Figure 1, we compare the stacked  $Y_{500}$  in our family of mock cluster catalogs to a “perfect” cluster catalog that has been calibrated according to Rozo et al. (2009). The “perfect” catalog uses a single calibration and does not contain any of the systematics we discuss in Section 2.2 and is identical to the model the Planck team used to compare to the data (Aghanim et al. 2011a). In each panel, the solid black line shows the average ratio (over multiple mock realizations) for models which apply the fiducial maxBCG values for calibration, mis-centering, purity, and mass scatter individually (as described at the end of Section 2.2). The grey bands show the range of models using the 1 and 2  $\sigma$  uncertainties on those parameters. Dotted-lines show more general models (e.g., 70%



purity independent of mass). We also show the Planck data presented in Aghanim et al. (2011a). We do not show redshift scatter and completeness since we found them to have negligible effect.

Systematic uncertainties ( $2\sigma$ ) in the mass-richness calibration result in a  $\sim 50\%$  range in the model  $Y_{500}$  measurements. This is because the  $Y_{500}$  values from our perfect catalog are calculated from a single mass calibration, while the model  $Y_{500}$ s are calculated using the masses drawn from the calibration including 1 and 2  $\sigma$  uncertainties. The figure indicates that the magnitude of the bias generated from uncertainty in the calibration of the mass-richness relation appears not to have a strong mass-dependence.

Mis-centering suppresses (biases low) the model  $Y_{500}$ s over the entire mass range, with the largest effect at low mass ( $\sim 25\%$  suppression). This can be understood from the convolution of the Planck beam ( $\sim 7'$ ) and the centering offsets which are on average  $\sim 3'$  at the median redshift of the optical sample. The offsets are large compared to the Planck beam ( $\sim 7'$ ), which blurs out the SZ-signal after the convolution. The impact of this effect increases to  $\sim 25\%$  at low mass, since the maxBCG mis-centering fraction is mass dependent.

Impurities suppress (biases low) the amplitude of the model  $Y_{500}$ s by introducing pure noise into the SZ maps. As also noted by Aghanim et al. (2011a), high levels of impurity would be required to explain the discrepancy with the data. Just as important, the weak-lensing calibration of the mass-richness relation would also be affected by large impurities which would lead to an enhancement in the mass-richness relation. Since  $Y_{500} \sim M^{\frac{2}{3}}$ , high impurities could even cause the observed SZ signal to be enhanced compared to the systematics-free case (something neither we nor Planck detect). Accurate modeling of the impact of impurities on  $Y_{500}$  requires simulating its effect on the weak-lensing calibration of the optical catalog.

The stated uncertainty in mass scatter (Rozo et al. 2009) does not have a significant impact on the SZ signal recovered using a maxBCG-like catalog. However, the same can not be said for the sub-sample which has an X-ray luminosity distribution similar to that of the MCXC (blue lines in the bottom panel of Figure 1 and see Section 2.4). The maxBCG/MCXC-like mocks contain clusters selected on their X-ray luminosity in order to match the real MCXC-maxBCG data used in the Planck analysis (Piffaretti et al. 2011; Aghanim et al. 2011a). In doing so, we unavoidably choose from the bright tail of the luminosity distribution in the lower richness bins (see Section 2.4). As a result, in our lowest richness bin the mean cluster mass for the MCXC-maxBCG subsample is 70% higher than the mean of the full maxBCG sample. Since  $Y_{500} \sim M^{\frac{2}{3}}$ , we see the expected behavior that the signal is enhanced by  $>250\%$  at low-richnesses. The effect goes away at high richnesses since most of the clusters in those bins are included in the sub-sample.

### 3.1. Simulating Planck-maxBCG Joint Analysis

Figure 2 compares the Planck results to our models. The Planck data (error bars) are the same in both panels from Aghanim et al. (2011a). The solid blue lines shows the single naive perfect model based on either the

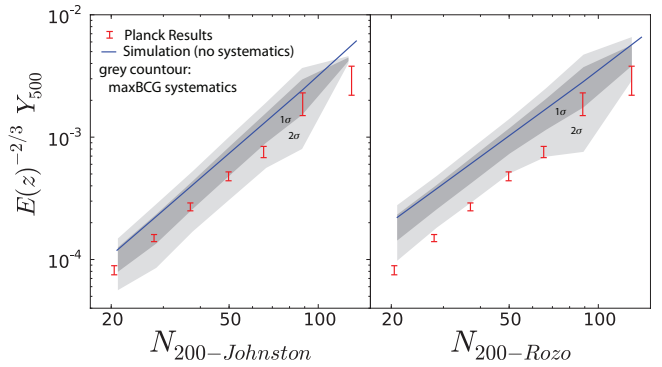


FIG. 2.— The Planck data (error bars) compared to the single perfect model used in (Aghanim et al. 2011a) (blue line) and to the range of models (grey bands) after jointly combining all of the individual systematic effects seen in Figure 1. The naive perfect model predicts higher (on average)  $Y_{500}$  values compared to the models which include catalog systematics. The data are consistent with our model predictions within the one (two)  $\sigma$  levels on the optical systematics for the Johnston (Rozo) mass calibration.

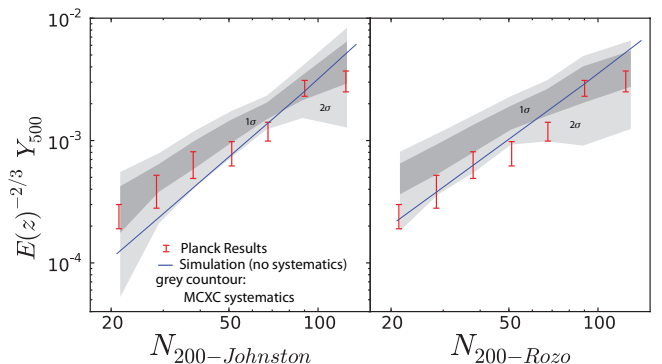


FIG. 3.— The Planck data for the maxBCG/MCXC X-ray sub-sample (error bars) compared to the single perfect model used in (Aghanim et al. 2011a) (blue line) and to the range of models (grey bands) after jointly combining all of the individual systematic effects seen in Figure 1. While the perfect model is the same as in Figure 2, the grey bands here include the bias seen in Figure 1 (bottom), which is caused after sub-sampling clusters based on their X-ray luminosities to match the observed data. The naive perfect model predicts lower (on average)  $Y_{500}$  values compared to the models which include catalog systematics. The data are consistent with our model predictions at the one (two)  $\sigma$  levels on the optical systematics for the Johnston (Rozo) mass calibration.

Johnston (left) or Rozo (right) mass calibration in the absence of systematics (Aghanim et al. 2011a). The gray bands show model predictions based on our Monte-Carlo mock cluster catalog realizations which include all of the maxBCG optical catalog properties, uncertainties, and systematics shown in Figure 1 and which were applied in the original weak-lensing richness mass calibrations. While the Planck data are statistically inconsistent with the naive perfect model prediction, they lie at the lower edge of the models which include the  $\sim 1\sigma$  and  $\sim 2\sigma$  systematic uncertainties (for the Johnston and Rozo mass calibrations respectively).

### 3.2. Simulating maxBCG-MCXC Joint Sample

Figure 3 shows our prediction for the MCXC sub-sample of the maxBCG catalog compared to the Planck data. As described in Section 2.4 our mock catalog includes the optical systematic effects and an X-ray lu-

minosity distribution that matches the real data. As expected from Figure 1-bottom, we see a bias in the predicted  $Y_{500}$  with decreasing richness. We understand these results in terms of a Malmquist-like bias where the X-ray sub-sample preferentially contains brighter (and thus more massive clusters) in the lower richness bins, thereby raising the stacked SZ signal above the prediction for no-systematics case (blue line). The Planck observations lie inside the lower edge of the models which include the 1 and  $2\sigma$  systematic uncertainties for Johnston and Rozo mass calibrations respectively.

#### 4. DISCUSSION

The Planck team reported that the stacked SZ signal around optical clusters lies well below the single model expectation which does not include the optical catalog systematic uncertainties. On the other-hand, they find that the observed stacked  $Y_{500}$  values around an X-ray limited sub-sample are consistent with the naive optical model. They concluded that the gas properties of clusters appear to be more stably related to each other than the gas-to-optical properties of clusters (Aghanim et al. 2011a). In this work, we reach a fundamentally different conclusion: the  $Y_{500}$  values observed by Planck are consistent with the model predictions for both the entire cluster sample and the X-ray sub-sample (to within the  $1\sigma$  optical systematic uncertainties and for the Johnston et al. 2007 mass calibration). Not only do we argue that there is no significant discrepancy between the models and the observed Planck stacked  $Y_{500}$  values around optical clusters, but we also argue that the optical and X-ray selected sub-samples simultaneously agree

with model predictions. For instance, we can apply a single mass-richness calibration to the data and fit the predicted  $Y_{500}$  models in Figures 2 and 3 simultaneously. However we do not pursue a joint SZ-optical mass calibration here, as it is beyond the scope of this work.

We find that the dominant source of optical systematic uncertainty comes from the mass calibration, which alone can account for most of the original discrepancy noted by Aghanim et al. (2011a). Impurities and centering errors combine to bias the model predictions towards lower  $Y_{500}$  for the optical samples while mass scatter biases the predictions high for low richness systems in the X-ray limited subsample. When fully accounted for, these systematics allow for models which are matched by the observed data for both the optical and X-ray cluster sub-samples in the Planck data. The range on the acceptable models is quite large and we note that the SZ-optical scaling laws cannot be precisely characterized using this type of stacking until the optical systematics improve (specifically mass calibration and its scatter).

This work highlights the importance of multi-wavelength studies of cluster properties as a source of cross-checks and a calibration. It is clear that optical systematics cannot be ignored and future analysis of stacked clusters should be done using Monte Carlo analysis to include a larger suite of systematic errors.

**Acknowledgments:** This work was supported through DoE Grant DE-FG02-95ER40899. In addition, we are grateful for the support of the NSF-funded Michigan AGEP Alliance program. L. Shaw acknowledges the support of Yale University and NSF grant AST-1009811.

#### REFERENCES

- Ade, P. A. R., et al. [Planck Collaboration] 2011a, *A&A*, 536, A8  
Ade, P. A. R., et al. [Planck Collaboration] 2011c, *A&A*, 536, A11  
Aghanim, N. et al. [Planck Collaboration] 2011a, *A&A*, 536, A12  
Arnaud, M., Pratt, G. W., Piffaretti, R., Bhringer, H., Croston, J. H., & Pointecouteau, E. 2010, *A&A*, 517, A92  
Birkinshaw, M. 1999, *Phys. Rep.*, 310, 97  
Bode, P., & Ostriker, J. P. 2003, *ApJS*, 145, 1  
Bonamente, M., et al. 2011, arXiv:1112.1599  
Carlstrom, J. E., Holder, G. P., & Reese, E. D. 2002, *ARA&A*, 40, 643  
Cunha, C., et al. 2009, *Phys. Rev. D.*, 79, 63009  
Draper, P., Dodelson, S., Hao, J., & Rozo, E. 2011, arXiv:1106.2185  
Duffy, A. R., Schaye, J., Kay, S. T., & Dalla Vecchia, C. 2008, *MNRAS*, 390, L64  
Dunkley, J., et al. 2009, *ApJS*, 180, 306  
Herranz, D., Sanz, J. L., Hobson, M. P., Barreiro, R. B., Diego, J. M., Martinez-Gonzalez, E., & Lasenby, A. N. 2002, *MNRAS*, 336, 1057  
Johnston, D. E., et al. 2007, arXiv:0709.1159  
Koester, B. P., et al. 2007a, *ApJ*, 660, 239  
Koester, B. P., et al. 2007b, *ApJ*, 660, 221  
Komatsu, E., et al. 2010, arXiv:1001.4538  
Marriage, T. A., et al. 2011, *ApJ*, 737, 61  
Melin, J., Bartlett, J. G., & Delabrouille, J. 2006, *A&A*, 459, 341  
Melin, J., Bartlett, J. G., Delabrouille, J., Arnaud, M., Piffaretti, R., & Pratt, G. W. 2011, *A&A*, 525, A139  
Miller, C. J., et al. 2005, *AJ*, 130, 968  
Motl, P.M. Hallman, E.J. and Burns, J.O. and Norman, M.L., 2005, *ApJ*, 623, L63  
Nagai, D. 2006, *ApJ*, 650, 538  
Piffaretti, R., Arnaud, M., Pratt, G. W., Pointecouteau, E., & Melin, J. 2011, *A&A*, 534, A109  
Rasia, E., Mazzotta, P., Evrard, A., Markevitch, M., Dolag, K. and Meneghetti, M. 2011, *ApJ*, 729, 45  
Roza, E., et al. 2009, *ApJ*, 699, 768  
Rykoff, E.S., et al. 2008, *Phys. Rev. D.*, 79, 63009  
Sanderson, A. J. R., Edge, A. C., & Smith, G. P. 2009, *MNRAS*, 398, 1698  
Sehgal, N., et al. 2011, *ApJ*, 732, 44  
Shaw, L. D., Holder G. P., & Bode, P. 2008, *ApJ*, 686, 206  
Sheldon, E. S., et al. 2009, *ApJ*, 703, 2217  
Sunyaev, R. A., & Zeldovich, Y. B. 1972, *Comments on Astrophysics and Space Physics*, 4, 173  
Vanderlinde, K., et al. 2010, *ApJ*, 722, 1180  
Vikhlinin, A., et al. 2009, *ApJ*, 692, 1060  
Williamson, R., et al. 2011, arXiv:1101.1290  
Wu, H.Y., et al. 2010, *ApJ*, 713, 1207